



Universidad
Zaragoza

Trabajo Fin de Máster

Métodos de seguimiento celular en imágenes
de cultivos 3D

Cell tracking image-based methods for
analysis of 3D cultures

Autor/es

Esther Tomás González

Director/es

José Manuel García Aznar
Carlos Borau Zamora

ESCUELA DE INGENIERÍA Y ARQUITECTURA

2017



DECLARACIÓN DE AUTORÍA Y

(Este documento debe acompañar al Trabajo Fin de Grado TFG)/Trabajo Fin de Máster (TFM) cuando sea depositado para su evaluación).

D./D^a. Esther Tomás González,

con nº de DNI 14278079R en aplicación de lo dispuesto

en el art. 14 (Derechos de autor) del Acuerdo de 11 de septiembre de 2014, del Consejo de Gobierno, por el que se aprueba el Reglamento de los TFG y TFM de la

Universidad de Zaragoza,

Declaro que el presente Trabajo de Fin de (Grado/Máster)
Máster, (Título del
Trabajo)

Métodos de seguimiento celular en imágenes de cultivos 3D

, es de mi autoría y es original, no habiéndose utilizado fuente sin ser citada debidamente.

Zaragoza,

Fdo: Esther Tomás González

AGRADECIMIENTOS

Agradecer en primer lugar el apoyo y consejo de mis directores, que me han guiado a lo largo de este proyecto. A Manu por su confianza, respaldo y acogida desde el primer momento y a Carlos por compartir todos sus conocimientos y por su ayuda más técnica. Agradecer al Consejo Europeo de Investigación (ERC) que ha financiado el trabajo a través del Proyecto ERC-2012-StG 306571 junto con la Prueba de Concepto IMAGO, con referencia GA nº 737543.

Desde aquí quisiera dar las gracias también a todas las personas del grupo M2BE, y al ‘Center for Medical Physics and Technology of Erlangen’ quienes me han prestado las imágenes de sus experimentos desinteresadamente.

A las personas con las que he compartido el día a día en la oficina: Cris, Yago, Sandra, Javi y Nieves, por dejarme aprender de su trabajo, mostrarme cómo funciona un laboratorio, cómo se realizan los experimentos, prestarme su tiempo y hacerme ver cuáles son sus necesidades y cómo un ingeniero puede complementar el trabajo que ellos realizan.

Destacar a mi gran compañera de laboratorio y de fatigas en general, Vanesa, con la que he compartido toda mi andadura universitaria y con la que espero seguir sumando momentos.

A todos los compañeros del máster que se han convertido en grandes amigos y pilares fundamentales. Ellos han hecho que la estancia en Zaragoza haya sido una gran aventura, la cual repetiría sin ninguna duda.

No quisiera olvidar a mi familia, los que siempre están al pie del cañón. Los que se interesan día a día por entender qué es “eso que yo hago”. También a los que en su día me inculcaron que el espíritu de lucha puede llevarte a conseguir lo que te propongas pero que hoy no pueden compartir esa lucha conmigo.

A mis padres a los que les debo todo, gracias por vuestro esfuerzo para que hoy pueda estar aquí. Y muy en especial a mi hermano, Jorge, mi gran referente y ejemplo a seguir, por sus consejos y sus largas conversaciones a pesar de los kilómetros.

A Emilio, por entenderme y respetar mis decisiones, por acompañarme en los buenos y malos momentos durante todo este camino y darme todo su cariño.

RESUMEN

Métodos de seguimiento celular en imágenes de cultivos 3D

La migración celular describe el movimiento propio de las células que les permite desplazarse a través de los tejidos. Este proceso es inherente a todos los organismos multicelulares y a través de él, pueden explicarse múltiples mecanismos fisiológicos como la homeostasis, la respuesta inmunológica, la regeneración de tejido o la metástasis del cáncer entre otros.

Hasta hace unos años el análisis de imágenes de microscopio se realizaba de manera manual y suponía un trabajo duro y tedioso, y cuyos resultados estaban sujetos a la interpretación del investigador. En las últimas décadas el análisis de imagen y la cuantificación computacional han permitido agilizar y estandarizar dichos análisis, aumentando pues drásticamente la cantidad y la calidad de la información recolectada.

Uno de los pasos esenciales para el análisis del movimiento celular en imágenes de microscopio es la detección y seguimiento de las mismas a lo largo del tiempo. Muchos son los algoritmos que se han desarrollado para realizar el tracking en imágenes con fluorescencia, confocal y cultivos 2D, sin embargo, los cultivos 3D, los cuales son biológicamente más relevantes, siguen siendo una tarea pendiente que requiere de un procesamiento más complejo.

En este proyecto se han implementado algunas propuestas de métodos de seguimiento celular orientadas a imágenes en 2D, pero obtenidas de un cultivo en 3D. Estas imágenes son adquiridas con un microscopio de luz convencional en modo contraste de fases en el que no se utiliza ni fluorescencia ni tinciones, por lo que, debido a dicha tridimensionalidad, se generan halos, desenfoque y otros artefactos que dificultan el análisis.

Todos estos algoritmos han sido incluidos en una plataforma de análisis de imagen semiautomática desarrollada en Matlab de la cual, por medio de modelado y análisis estadístico se obtienen los parámetros más representativos del movimiento celular.

Este trabajo fin de Máster está enmarcado dentro de una “Proof of Concept” denominada IMAGO, derivada del proyecto Europeo INSILICOCELL. El objetivo último de IMAGO es prestar un servicio online de análisis de imagen biomédica, entre cuyas principales utilidades está la cuantificación del comportamiento celular y la extracción de los principales parámetros de migración, generando un informe para el usuario con los resultados más significativos.

ABSTRACT

Cell tracking image-based methods for analysis of 3D cultures

Cell migration is the orchestrated movement of cells that allows them moving through tissues. This process is inherent to all multicellular organisms and can explain multiple physiological processes such as homeostasis, immune response, tissue repair and cancer metastasis among others. The importance of these events makes it necessary to extract relevant information from molecular/cellular experiments.

The manual analysis of microscopy images has historically required long and working and the results were subject to researcher's interpretation. However, in recent years, image analysis and computational quantification have allowed to streamline and standardize analyses, thus increasing the quantity and quality of data.

One of the essential steps for analyzing cell movement in microscopy images is their detection and tracking over time. Many algorithms have been developed to track fluorescent, confocal and 2D culture images, but 3D cultures, which are biologically more relevant, remain as a pending task requiring more complex processing.

In this project, some proposals have been implemented for cellular tracking oriented to very particular images in which we try to follow the cell which is cultivated in a 3D medium from a plane image. These images are taken with a conventional light microscope in phase contrast mode in which no fluorescence or staining is injected, which, due to the 3D nature, creates halos, blur and other artifacts that difficult a proper analysis.

All algorithms are included in a semi-automatic image analysis platform developed in Matlab from which a report of cell dynamics is obtained, including statistical analysis and models.

This final master's project is framed the project IMAGO, derived from the European Project INSILICOCCELL, which aim is to provide an online service for biomedical image analysis. One of IMAGO's main functionalities is the quantification of cell behavior and the generation of user-oriented reports.

Contenido

AGRADECIMIENTOS.....	3
RESUMEN	5
Métodos de seguimiento celular en imágenes de cultivos 3D.....	5
ABSTRACT	7
Chapter 1	2
INTRODUCTION	2
1.1. CELL MIGRATION	2
1.2. MICROSCOPY IMAGE ACQUISITION TO ANALYSE CELL MIGRATION.....	4
1.3. CELL TRACKING: STATE OF ART	5
1.4. MOTIVATION AND OBJETIVES.....	6
Chapter 2	8
METHODS	8
2.1. NUMERICAL IMPLEMENTATION OF TRACKING METHODS	8
2.2. STATISTICAL ANALYSIS.....	15
2.3. PLATFORM IN USE	16
Chapter 3	17
RESULTS.....	17
3.1. COMPARISON BETWEEN TRACKING METHODS.....	18
3.2. COMPARATIVE STUDY DEPENDING ON CELL TYPE	20
3.1. DIFFERENCES BETWEEN 2D AND 3D IMAGES.	25
Chapter 4	27
SUMMARY AND CONCLUSIONS.....	27
References.....	29

Chapter 1

INTRODUCTION

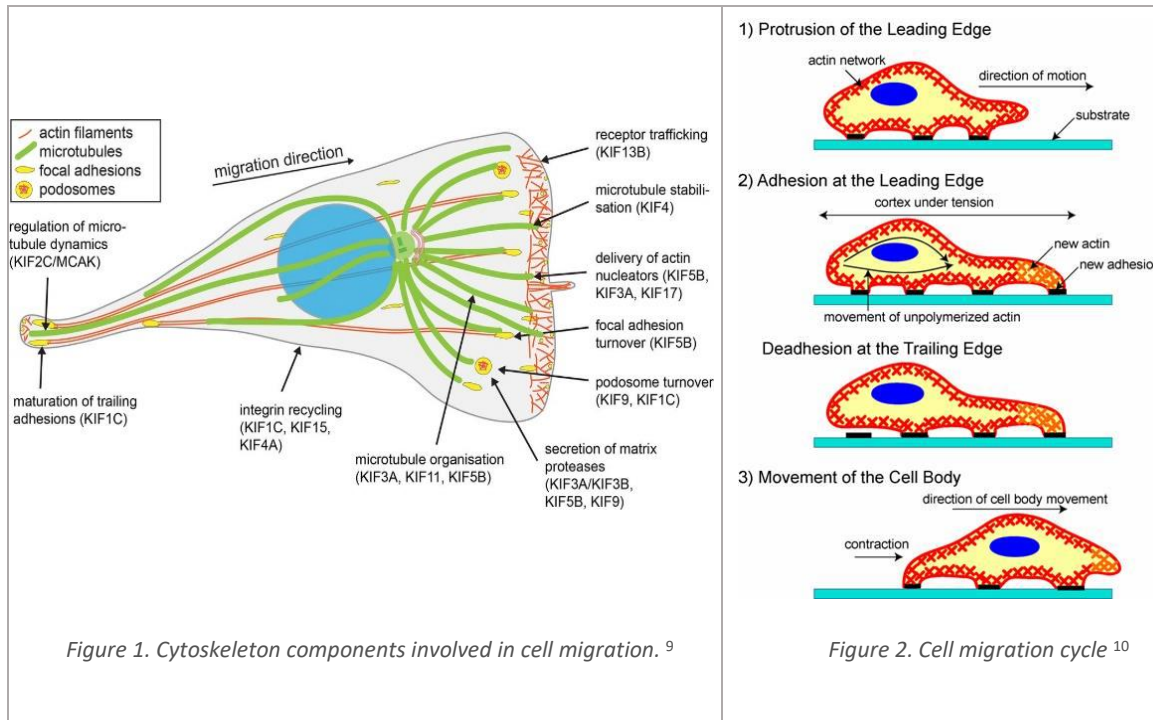
1.1. CELL MIGRATION

Cell migration is a basic cell function that establishes and maintains the proper organization of multicellular organisms. The ability to migrate allows cells to change their position within tissues or between different organs, it is a central event in physiological processes such as embryonic development¹, immune responses², wound healing³ or tissue homeostasis but also in pathological processes including cancer metastasis⁴. Understanding how and why all these processes occur, can radically change therapeutic approaches for treating diseases, biological structure regeneration or artificial tissues preparation⁵.

One of the most important parts of the cell in terms of cell migration is the cytoskeleton. The cytoskeleton consists on a system of filaments extending from the cell nucleus to the surface. Three families of proteins make up the cytoskeleton: microtubules, intermediate filaments and actin filaments, all of which are described Figure 1. These proteins contribute to intracellular transport and the control of cell motility through mechanotransduction⁶. However, migration through interstitial tissue is a multiscale process resulting from a physico-chemical balance between the cell and its surrounding. The non-cellular part of the tissue is the extracellular matrix (ECM).

Cell migration can be described as a cyclic process in general terms as shown in Figure 2. The initial response of a cell to a migration-promoting agent is to polarize and extend protrusions in the direction of migration⁷. The supramolecular complexes through the actin-cytoskeleton is anchored to the ECM are called focal adhesions (FAs). The cell moves forward over the FA, and they are disassembled at the rear of the cell, allowing it to detach and contract. Directional migration is usually initiated by extracellular cues such as gradient of growth factors or chemokines. However, it can also be indicated by mechanical forces , such as cell stretching

or fluid flow, ECM proteins like collagen and fibronectin, the topography and mechanics of the ECM and electrochemical gradients⁸.



The migration cycle can vary considerably depend on the type of the cell and the microenviromental culture conditions (2D Vs 3D)¹¹. Highly protrusive or blebbing cells (for example, lymphocytes and some cancer cells) are at one extreme and seem to migrate using weak adhesions. On the other hand, spread cells such as fibroblasts and endothelial, are at the opposite and have many large adhesions. To sum up, although cell migration is considered a cyclic process, is the direct coupling between the cell and the ECM at integrin-based adhesion sites that allows the cell to mechanically sense their physical surroundings and adjust migration mechanisms.

Mechanisms regulating cell motility have been extensively studied in 2D but the microenvironmental conditions in living tissues are better addressed by 3D conditions. The environment in 2D lamellipodial migration is isotropic, spatially and temporally homogeneous, and generally similar from lab to lab, perhaps that is why the substrate has often been ignored although its mechanics properties, surface topography, stiffness and adhesivity have been explored¹². Furthermore, it has been proven that cellular mechanics¹³, as well as migratory mechanisms diverge profoundly when the dimensionality switches. For example, in 3D, fibroblast interact with collagen through dendritic extensions to detect changes in tissue mechanics and hence, exhibit distinct patterns of migration and remodeling in a contextual dependent manner. In planar substrates, fibroblasts are not able to form the dendritic structures, they modulate their cytoskeletal function in response to surface mechanics by acto-myosin activity, but they have little capacity to modulate the overall molecular organization and mechanical properties of the ECM-coated surfaces¹⁴. In the case of melanoma cells, they tend to adopt rounded morphologies with protuberant membrane blebs when embedded in a 3D collagen matrix while on hard surfaces, these cells adopt elongated and flat morphologies¹². Because of all this, even though the 2D study has provided great knowledge about cell migration, the 3D study is becoming more and more essential, leading current and future lines of research.

The recreation of real 3D local microenvironments requires microfluidic technology. In 2D culture chips or petri dishes, cells adhere to the surface and cannot move in a three-dimensional manner. Microfluidic chips allow the insertion of a gel inside, which serves as a scaffolding for cells to grow in a three-dimensional microenvironment. Microfluidic technology makes it possible to grow a few hundred cells in the devices compared to the thousands or millions that macroscopic cultures offer. That allows to do studies with individual and isolated cells, being able to control either the extracellular matrix, the cells themselves or the chemical gradients independently and in a common scenario. The culture chips are manufactured with PDMS and allow multiple geometries to be adapted to the type of assay.

1.2. MICROSCOPY IMAGE ACQUISITION TO ANALYSE CELL MIGRATION

Since the earliest examination of cellular structures, scientists have been observing cells using optical microscopy also called light microscopy. Light microscopy acquisition in cell cultures, is essentially a trade-off between a high signal-to-noise ratio and the damage of the sample under observation. When selecting which system to use for imaging living cells, one should consider three main concepts: sensitivity of detection, speed of acquisition, and the cell's health on the microscope stage. The sensitivity of the camera will be vital, because the more sensitive the detector, the lower the illumination intensity needed which is essential to avoid photodamage in cells.¹⁵ Regarding timing, it is important to know the necessary temporal scale because it is crucial to maintain the sample in the same conditions throughout the whole experiment. For life-imaging, this is obviously the most important aspects: keeping cells in a proper environment to avoid mortality. In that sense, it is vital to control the temperature, humidity and CO₂. The aim of image acquisition is to reproduce as accurately as possible what is occurring in the culture to be quantified. The problem is that getting high spatial resolution to see fine structural detail and high temporal resolution to follow fast dynamical processes are mutually opposed. In other words, increased spatial resolution requires more measurements, take more time, and pumps more potentially damaging radiation into the specimen.

The most popular optical microscopy techniques, depending on the source of incident light are: white light, fluorescence and confocal. The first one is the simplest technique: the sample is illuminated by white light and the contrast in the image is caused by attenuation of the transmitted, reflected or refracted light in different areas of the sample. In the case of fluorescence, the specimen is illuminated with a specific wavelength light which is absorbed by the fluorophores causing them to emit light of longer wavelengths¹⁶. In this case, samples must be fluorescent, hence, for non-auto-fluorescent bodies such as cells, it is indispensable to express a fluorescent protein in the biological sample¹⁷. This involves doing a transfection process in the cells. Finally, confocal technique allows acquiring the most accurate images. The sample is illuminated by a powered laser light source point by point and eliminates light from unfocused planes, which furthermore allows creating z-stacks (focusing iteratively at different planes) that can be visualized in 3D. Figure 3 shows some examples of images taken with different optical microscopy techniques (For more information about microscopy acquisition techniques see supplementary material 1)

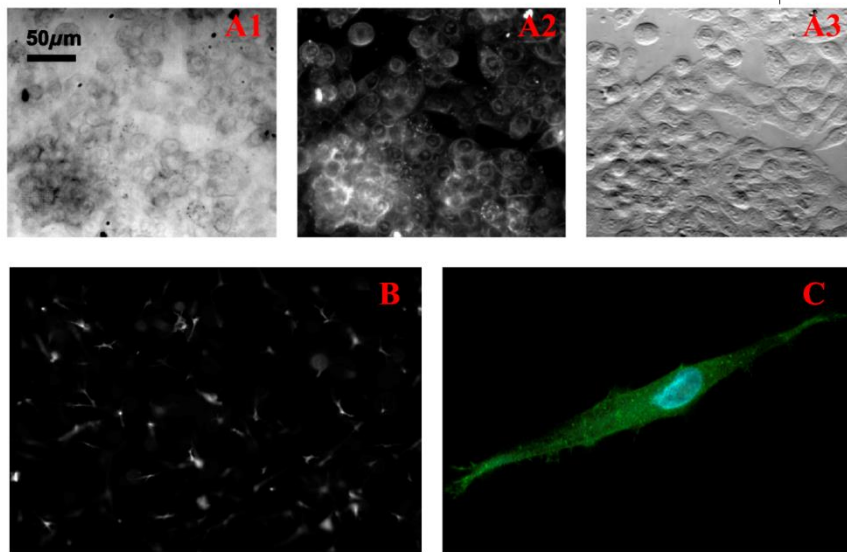


Figure 3. A) Experimental results for HeLa cell samples imaged with 20x, NA 0.4 objective white light microscopy with different contrast techniques: A1. Bright field; A2. Dark field; A3. Top-Bottom phase contrasts. (adapted from ¹⁸) B) Fluorescence image of 3D fibroblasts culture imaged with a Nikon D-Eclipse Microscope with a Plan Fluor 10X objective. C) Confocal image of human osteoblast imaged with 60x-Oil objective.

1.3. CELL TRACKING: STATE OF ART

The study of cell migration, as well as intracellular transport, viral infection, gene transcription, genome maintenance and other dynamics process occurring in the cell membrane, cytoskeletal filaments or focal adhesion require a spatial-temporal study in which detecting and tracking these particles is essential. Manual annotation of the image data is not feasible, and computer algorithms are needed to perform the task. Bioimage developments in last decades have allowed acquiring more precise images and with higher resolution, but also to analyze them in a more automatic, consistent and efficient manner. This project is focused on cell migration whose accurate quantification could lead to a better mechano-biological understanding of cell behavior under different conditions. This task has many challenges including the generally low contrast and high noise levels in the images (due to the 3D nature of the medium), the varying density of cell populations due to cell division, cells entering or leaving the field of view, the crossing of trajectories, the possibility of cells touching each other without enough image contrast to distinguish them, or scattered cells that might not be interesting for the experiment because they died, got stuck and so on.

Regardless of the type of image acquired, tracking methods can be classified into two broad categories: tracking by detection and tracking by model evolution^{19,20}. In both of them there are two main steps: segmentation (spatial aspect) and cell association (temporal aspect). Segmentation is the process of dividing an image into meaningful parts. Segmentation process can be based on many methods ranging from the simplest ones like thresholding, fitting predetermined cell intensity profiles²¹, watershed transformation, deformable models²² or the combination of all of them²³ to the new and powerful methods such as machine or deep

learning²⁴⁻²⁶. After segmentation, the second step is cell association, it refers to the process of identifying and linking segmented cells from frame to frame. There are also many approaches to accomplish this, but it is usual to define the “nearest”, including in this concept intensity, area, volume boundary, axis, curvature, estimated displacement and other features. It is also common applying a template matching for non- deformable particles, using the gradient-vector flows, estimation of cell dynamics or using probabilistic schemes.^{27 28 29}

On the one hand, in tracking by detection methods, all cells detected in all frames and then the most likely cell correspondence between frames is determined. Its main benefit is the independence of both steps, which allows straightforward tracking of new cells entering the field of view as well as forward-backward spatiotemporal data association. On the other hand, in model evolution methods, cells are segmented and tracked simultaneously using the final result of each frame as the initial condition for the analysis of the following frame. These methods are popular for adapting morphological and behavioral clues into the model to deal with the topologically flexible practice of live cells.

Nowadays there are many public or private microscopy image analysis platforms (e.g. ImageJ, Fiji, CellTracker)^{30,31} which have implemented many cell tracking algorithms (e.g. IMARIS, icy, OracleBio, Wimasis). Some of them are only prepared to analyze 2D culture experiments and most of them only accept fluorescence experiments. Some others that work with cell migration in 3D, acquire images in many slices and make a reconstruction in order to perform a real tracking in 3D (that is, acquiring the z-component)³². However, to the best of our knowledge, none of them are thought to analyze 3D cultured cells via only 2D images, which is very interesting for use because, due to the architecture of experimental setup, the vertical component of the movement is usually negligible compared to horizontal one.

1.4. MOTIVATION AND OBJETIVES.

The study of cell migration can lead to great advances in understanding and treatment of certain diseases as seen in the previous sections. Further research in this area increasingly requires a more precise analysis of the situation. This analysis involves: reproduction in controlled situations of the cellular environment; a high resolution and cell-friendly acquisition of images; automatic, accurate and reliable post-processing of images; and also a tiny study of the data obtain from the assay.

The M2BE laboratory carries out different kinds of experiments mainly using cardiac, epithelial³³, fibroblast^{34,33}, osteoblast³⁵ and stem cells. These experiments are 4D (3D+time) *invitro* cultures to study the dynamic behavior of cells in different conditions. Each experiment usually takes 24-48 hours in order to observe cell movements and morphological changes. To that end, image acquisition is performed in a white light microscope with phase-contrast methodology, normally taking one image every 20 minutes. One example is shown in Figure 4B in comparison with other techniques (seen Figure 4A, 4C). We have tried to avoid the use of fluorescence because it is unclear to what extent cell movement is affected by the transfection process. Furthermore, due to its simplicity (clear signal vs. totally black background) there are already many available tracking methods. In addition, so far there is no confocal microscope

capable of performing a 3D scan with cultures long enough to track cells in motion without burning them.

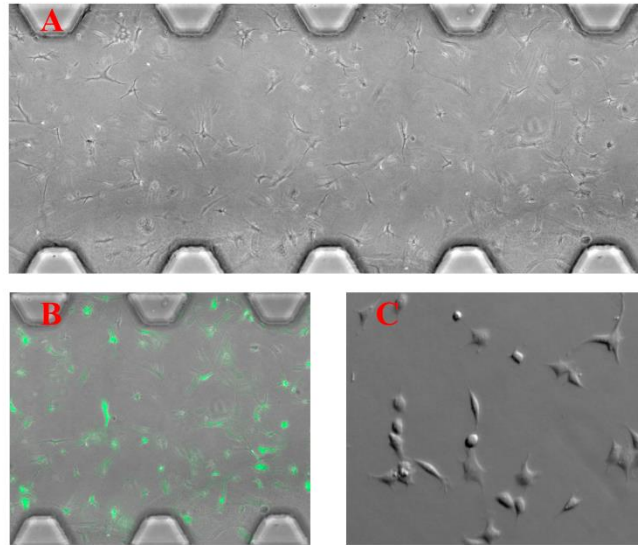


Figure 4. A) 3D fibroblast experiment contrast phase imaged with a Nikon D-Eclipse Microscope with 10X objective. B) Same experiment as A with fluorescence image superposed acquired with Plan Fluor 10X objective. C) 2D assay of mouse fibroblast

The main objective of this project is to compare, by means of statistical studies, the accuracy of different tracking methods for cells of different type in order to classify and include them in the IMAGO platform. It is worth reminding that the main goal of IMAGO is to provide an online platform to request microscopy image analyses and develop high quality reports.

The detailed tasks of the present work are as follows:

- To explore different cell tracking algorithms used for white 2D light microscopy imaging in 3D cultures.
- To develop new cellular tracking methods.
- To compare the different selected algorithms against the results of a manual tracking (ground truth).
- To test every method with different cells types as well as for different types of images or cultures (2D vs 3D).
- To integrate the algorithm in the existing platform that serves as a user interface in order to obtain a complete cell migration analysis.

All the existing and novel developed codes are written in Matlab.

Chapter 2

METHODS

2.1. NUMERICAL IMPLEMENTATION OF TRACKING METHODS

This chapter describes step by step four methods which have been implemented and some of their variations. All of them are model evolution methods because of the flexible shapes, intensities and movements of cells in the images. The basic steps of the algorithms are the following:

- i. Selection: the user selects some cells of interest clicking their centroids in the first frame.
- ii. Pre-processing: input images are pre-processed to eliminate possible noise and highlight cells.
- iii. Cell-association: the new centroid of every cell is searched in the current frame, taking into account the information from the previous one.
- iv. Iteration: (iii) is repeated for every frame and cell. Those cells moving outside the boundaries or not fulfilling certain requirements are marked as lost and ignored in the subsequent steps.

CellMigration()

```
i) The user selects the centroid of cells in first frame  
ii) Read images and preprocessing of all frames (background)  
for frame 2 to NumberFrames  
    for n = 1 to Number Cells  
        iii) Get new centroid with cell association method  
    end  
end  
end
```

2.1.1. PREPROCESSING METHODS

Noise may be present in cell-culture images due to multiple factors such as condensation of the medium when the conditions of the experiment change (e.g. causing a fog in the sample) or the presence of unfocused planes that have no relevant information and produce halos. It is advisable to remove these unwanted artifacts before beginning to process the image, and highlight the parts which are of interest from the background. For this reason, a preprocessing of the image is required. In this section three different methods are proposed to enhance image quality as much as possible.

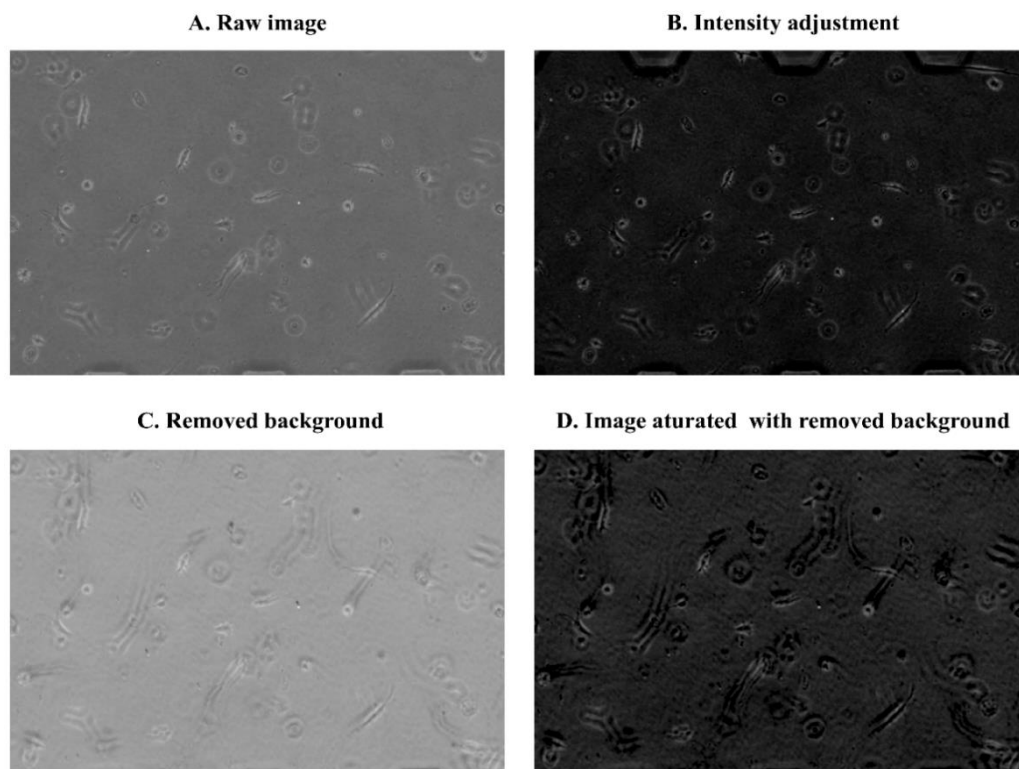


Figure 5. Preprocessing images in osteoblast assay. A) Raw image. B) Intensity profile adjusting. C) Image after subtracting the background. D) Image saturated after subtracting the background.

The simplest method is to adjust the range by saturating the intensities ends. This increases the contrast in the image by making interesting areas much more emphasized, as shown in Figure 5A. When talking about this preprocessing method, it will be assumed that the image is raw.

Another preprocessing method is the elimination of the background. Firstly, an average of each pixel over time is calculated and after that it is subtracted from the original image. The objective is that in those areas where the image has been static the value of the mean and the pixel of the original image is practically the same and when subtracted they are set to zero. On the contrary, in those areas where the image has had movement, that is to say, in those pixels where the cell has passed over, the mean and the original value will be different and therefore the subtraction will give us a value different than zero. The result of deleting the background of the image can be seen in Figure 5B. Hereafter referred to this method as BackG.

Finally, a saturation test is performed, so that after eliminating the background we only analyze the positive values and saturate negative ones to zero. The aim of all these methods is to mark all cells with high intensity values. This type of preprocessing has great advantages for certain kinds of images such as the one shown in Figure 5C where cells are fully distinguished with respect to the background. However, it is not convenient for images that are very dark originally, those that do not have constant background, for example those that have a halo of condensation or in which the movement of cells is very small. This pre-processing method will be named as BackSat.

2.1.2. ASSOCIATION CELL METHODS

Correlation based method.

Correlation weights the similarity between two signals. This concept can be applied for 2D signals, for example images. It is not usual that cells change their shape drastically in two consecutive frames. For this reason, it is possible to calculate the correlation between two frames to find the most similar areas. The idea of applying correlation to track cells is not new, other groups have already implemented correlation function for 2D signals³⁰. In that case they use bright field microscopy images with stain cells cultivated on 2D dishes. Taking this technique as a reference, an algorithm based on it has been developed, correlation based method.

This method saves in each frame not only the coordinates of the cell's center but also a cell-centered cropped window containing the cell's surroundings. This piece of the image will be used to find the best correlation on a bigger search area of the next frame. This area is adapted to the cell size and maximum possible displacement taking into account usual cell velocities.

This window is furthermore transformed with the aim of unifying all cellular intensities, since, even in the same image, some of them appear light, others dark, with halo, etc. This transformation has two main steps: first, the maximum intensity of the image is subtracted and the absolute value of this subtraction is calculated (image inversion); second, the image is blurred with a Gaussian filter and the difference between the inverted image and the filtered image is obtained, which helps to smooth the background noise. As shown in Figure 6 depending on the type and morphology of each cell, either cell edges or body are highlighted.

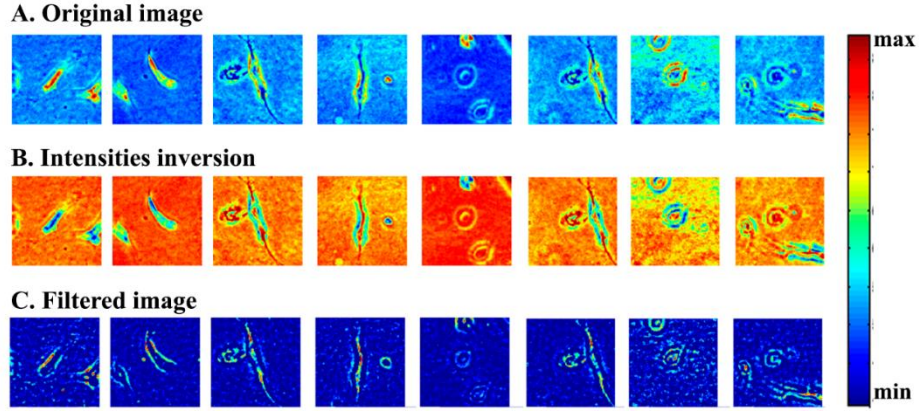


Figure 6. Steps of enhanced cell images. A) Original cell image. B) Intensity inversion (Subtract the maximum and get the absolute value) C) Filtered image with Gaussian filter.

After enhancing both images, template image (from previous frame) and search Image (from current frame), they are used to obtain a correlation. In order to do the correlation in a 2D signal it is necessary to calculate the Fourier Transform of both images among other operations. The output of the correlation in two dimensions is a matrix of the same size of the bigger image with the correlation value in each pixel. This value ranges from 0 (no correlation) to 1 (maximum correlation). The correlation weights the similarity between both images, so the biggest value would indicate the center of the cell in the new frame. The final step before taking the maximum in the correlation is filtering the resulting matrix with a Gaussian mask in order to get out of any punctual high value and to get rid of fast changes. Note that the method assumes that the morphological changes of cells between two consecutive frames are small enough to recognize the pattern. Figure 7 shows up to eight different cells (columns) and the subsequent image process step by step (rows). In addition, in supplementary material 2 a summary of the code is shown.

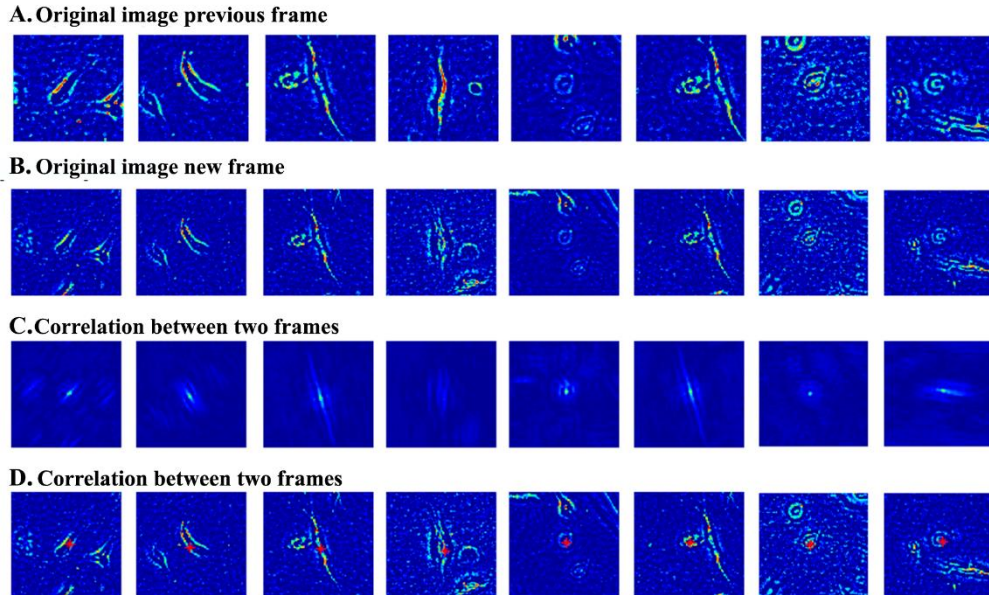


Figure 7. Steps for cell association in Corr (correlation based method). A) Template image in previous frame (t) centered in the selected centroid. B) Search area in actual frame ($t+1$). C) Correlation between A and B filtered with Gaussian filter. D) New centroid calculated from the maximum correlation in actual frame ($t+1$).

Iterative mass center based method.

In this case, once the cell centroid is selected in the first frame, its coordinates are the only information saved to analyze the next frame. A new centroid position is therefore found in the current frame (t), and this information is used to find a new centroid in the next one ($t+1$) and so on.

To find the centroid in $t+1$ a possible area of displacement (search window) is defined around the centroid found in t . The size of this window depends on the average cell size and the maximum expected velocity, so that it is big enough to find the cell but not too much to find other objects (e.g. other close cell). This window is enhanced following the same method described in the previous section (seen Figure 6).

$$x = \frac{\sum_{j=1}^M \sum_{i=1}^N i * I_{i,j}}{\sum_{j=1}^M \sum_{i=1}^N I_{i,j}}, y = \frac{\sum_{i=1}^N \sum_{j=1}^M j * I_{i,j}}{\sum_{i=1}^N \sum_{j=1}^M I_{i,j}} \quad [1]$$

N = number of rows
M = numbers of columns
 $I_{(i,j)}$ = image intensity
(x,y) = coordinates of mass center

After this process, mass (intensity) center is searched to set the cell centroid. Mass center is calculated as an average of coordinates weighted with the intensity of the image as described in formula 1, that is to say, those with greater intensity will have a greater weight. In this way a point will be obtained around the coordinates with greater intensity. This process is repeated in every frame for every cell in a loop. In each iteration, the search window is centered according to the new mass center. The loop stops when at least one of this conditions is fulfilled: i) the difference between two consecutive iterations is small enough, ii) the velocity obtained is bigger than a maximum set value (corresponding to normal velocities of cells), iii) the maximum number of iterations is achieved (the algorithm is not converging to a solution). The goal of this iteration loop is to find the point in the cell's center exactly and examine the whole possible cell. Figure 8 shows cell association in mass center based method. It is worth noting that the algorithm finds the maximum intensities, which in some cells correspond to their edges and not to their centroid. In any case, this feature doesn't change along the frames, so such cells are robustly tracked too. This iterative process is schematized as follows:

CellAssociation (MassCenter)

```
1. Load the coordinates in last frame

for i =1 to number of iterations or high displacement
|
|   2. Get window in actual frame around save coordinates
|   3. Get enhanced window
|   4. Calculate the mass center and save the coordinates
|   5. Calculate max displacement
| end
6. Save final coordinates for the cell in actual frame
```

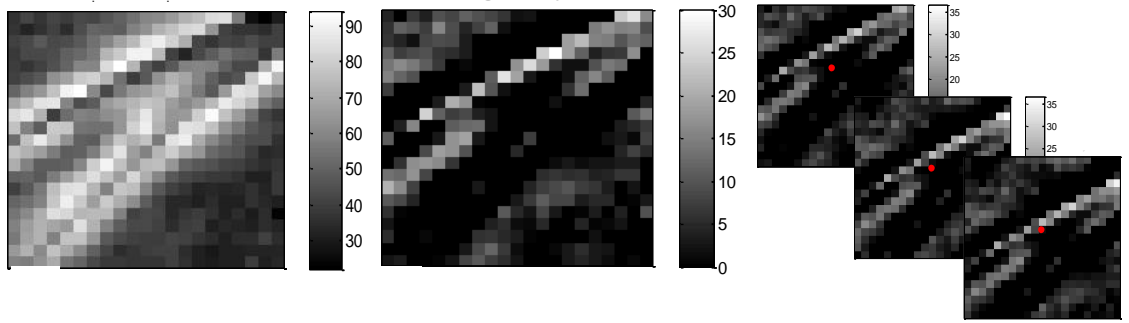


Figure 8. Steps for cell association in MC (iterative mass center) based method. A) Area of possible displacement of cell center in the frame. B) Enhanced image. C) Calculate the mass center iteratively.

Segmentation and correlation method.

This method, has been developed to make the most of all information in the previous frame to find the cell in the current one. In this way, it is important to emphasize cell area and shape to find it easier. In other words, the cell is segmented (binarized) before searching it on next frame but without losing the intensity information.

First of all, we increase the contrast in those images, which it is very low, by scaling the intensities. Secondly, we find the general shape of the cell in an area according to its size. For this purpose, the gradient of the image is obtained and dilated in order to highlight the great changes of intensity at the cells boundaries. The next step is to reconstruct the image³⁶, taking advantage of the fact that the cell centroid is already known. The reconstruction is conceptually a repetition of dilations in an image, called the marker image, until the contour of the marker image fits under a second image called the mask. In our case, the mask is a point in the center of the image because we know the cell is there and we try to adjust the image profile to that one. Figure 9 shows a 1D representation of a reconstruction process. After the reconstruction, a maximal region function is applied to connect those maximal zones which are separated for one or two pixels. These two main steps are represented in Figure 10C.

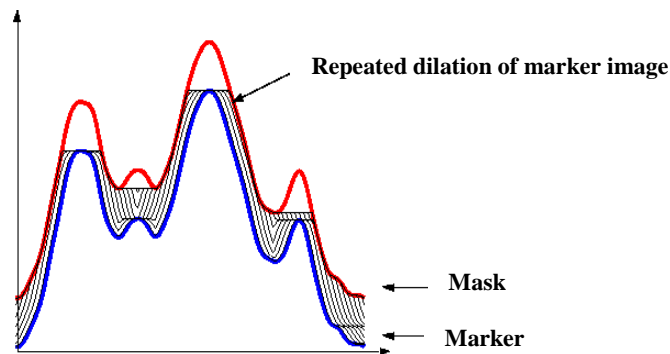


Figure 9. Representation of 1D reconstruction signal.

At this point an image with a very high intensity value in the area where the cell is located is obtained. This image is saved as a template to obtain the correlation with the search image. Now it is easier to segment the cell. This segmentation will provide a marker to perform a morphological reconstruction on the next frame.

In order to prepare the image in which the cell is being searched, a portion of the image is taken from the next frame around the calculated center of the cell taking into account the possible displacement of the analyzed cell. The same process described for the template image is performed as: intensity scaling, gradient, dilatation, reconstruction (but this time with the marker created from the segmentation) and a maximal region. The result of all this process is shown at figure 10E. The correlation is made between the template image and the search region, and then the maximum correlation is set as the new cell centroid, similarly to the previous method. A brief summary of the code is described in supplementary material 2.

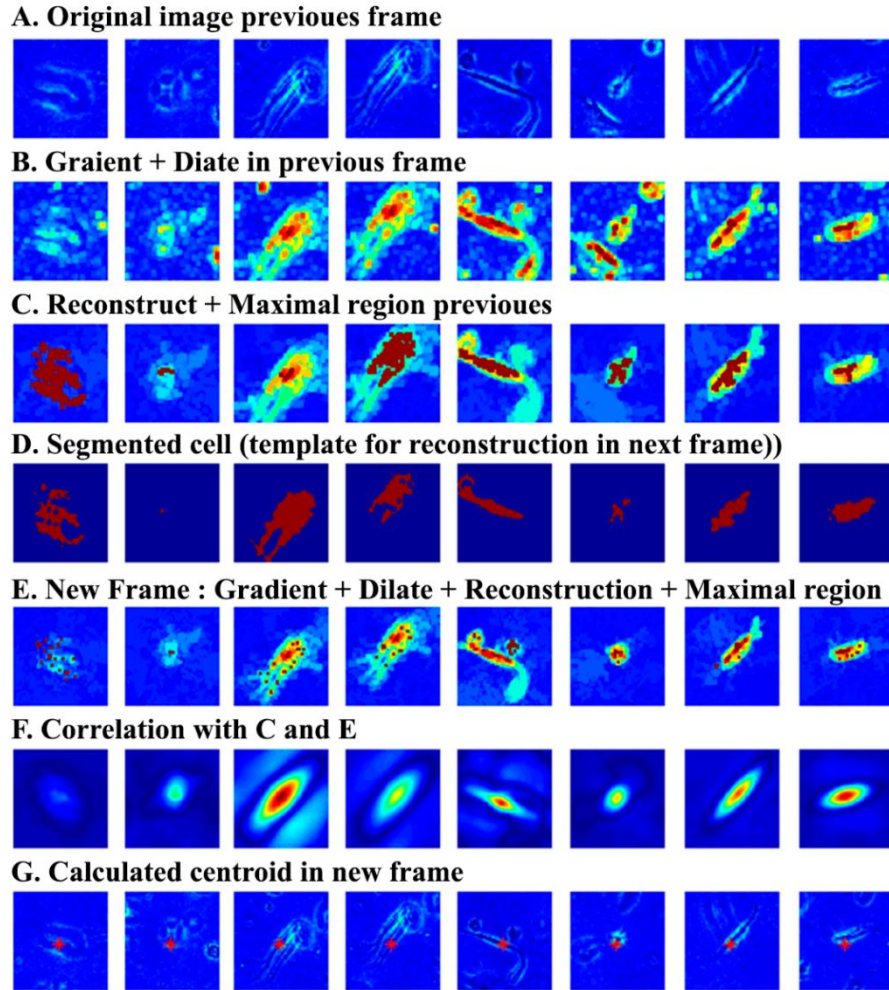


Figure 10. Steps for cell association in SegCorr (segmentation and correlation) based method. A) Raw cell image in previous frame. B) Gradient and dilatation of A. C) Morphological reconstruction and maximal region of B (Template Image). D) Segmentation. E) Gradient, dilate, morphological reconstruction with marker in D and maximal region in new frame (Search Image). F) Correlation between template and search images (C and E). G) New centroid calculated from de maximal of correlation. It is plotted in raw image new frame.

Segmentation, correlation and mass center method

The last implemented method is a mix of the previous ones. From the first step of image enhancing to the step of correlation does the same as the segmentation and correlation based methods. However, instead of finding the maximum correlation value, a mask with the higher correlation values (specifically from 70% to 100% of the maximum) is used on the search image to calculate the intensity mass center only from the masked pixels (which are supposed to belong to the cell). Figure 11 shows the new steps of the process and supplementary material 2 has a pseudo code of the method.

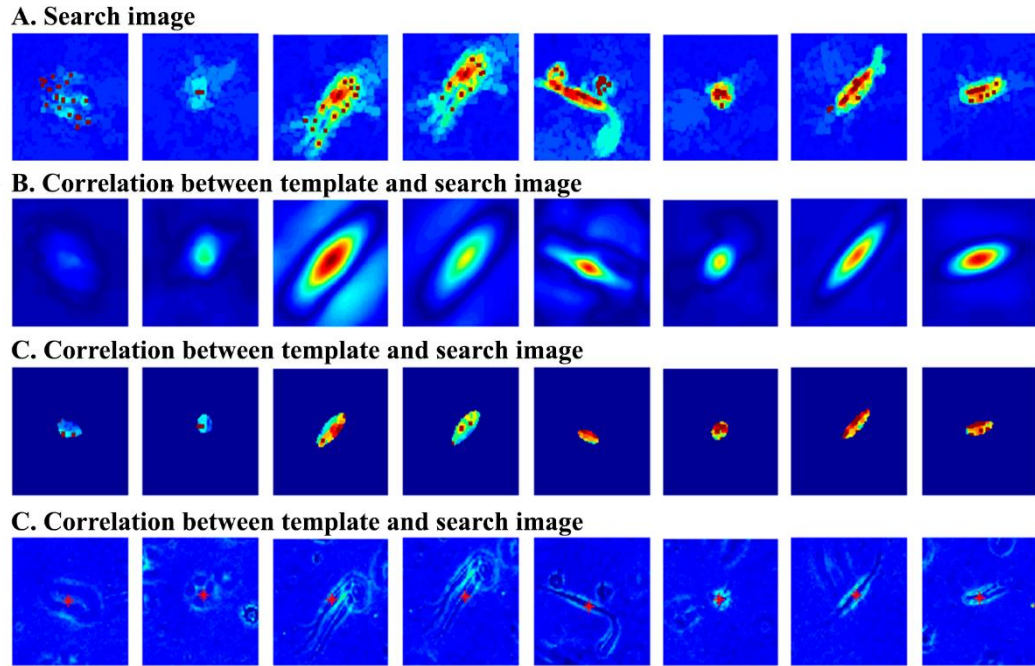


Figure 11. Last steps in SegCorrMC (segmentation, correlation and mass center) based-method. Previous steps are Figure 10 A, B, C, D. In this Figure: A) Gradient, dilate, reconstruction, maximal region in new frame. B) Correlation between Template image (Figure 10C) and search image (A). C) Search image with a mask of maximal correlation area. D) Mass center calculated with C plotted in raw new frame image.

2.2. STATISTICAL ANALYSIS

In order to analyze different methods objectively, a ground truth and a statistical method for comparing trajectories is necessary. Manual follow-up has been obtained in 12 migration assays by selecting between 6 and 12 cells in each of them. These twelve trials include stem, osteoblast, cardiac and epithelial cells (three assays repetitions of each type). In all the studies, 73 images were taken, comprising 24-hours periods. That is, one frame every 20 minutes. Once the manual path has been saved, same cells are tracked using all the developed methods. Afterwards, the error is obtained between every point of each cell trajectory and the ground truth by means of Euclidean distance. Because of the different sizes of cells, the error is

divided by the average cell size for each cell type. In other words, the error reflects how far the automatically calculated centroid moves away from that obtained manually in the form of a percentage of the cell. From each cell trajectory the point to point error, the average error, the maximum error and the deviation are obtained.

Comparison between error distributions is made, generally grouped by tracking methods but also by cell types, since the shape of the cells as well as their trajectories are very different and the best method for each could not be the same.

2.3. PLATFORM IN USE

It should not be forgotten that the final objective of tracking is to study cell migration. Tracking itself would be useless if it is not integrated into a platform allowing researchers to use it as a tool to obtain the most relevant parameters of cell movement. Therefore, these methods have been adapted and included into a semi-automatic analysis platform in which it is possible to choose the tracking method depend on your assays. This platform implemented in Matlab provides researches with important variables related to cell migration such as: cell area, length and number of cell's branches, migration direction, eccentricity, mean and effective velocities, diffusivity constants, persistence time and speeds, anisotropy index and so on. The supplementary documentation 3 shows a process of analysis of a complete migration test .

Chapter 3

RESULTS

This chapter is dedicated to the analysis of the results obtained when executing the different tracking methods. Comparisons of the trajectories will be grouped in different categories, first using all the data together and then divided by cell types. Lastly a comparison between images taken for a two-dimensional culture versus our 3D assays is presented. A visual example of path comparison is shown in Figure 12.

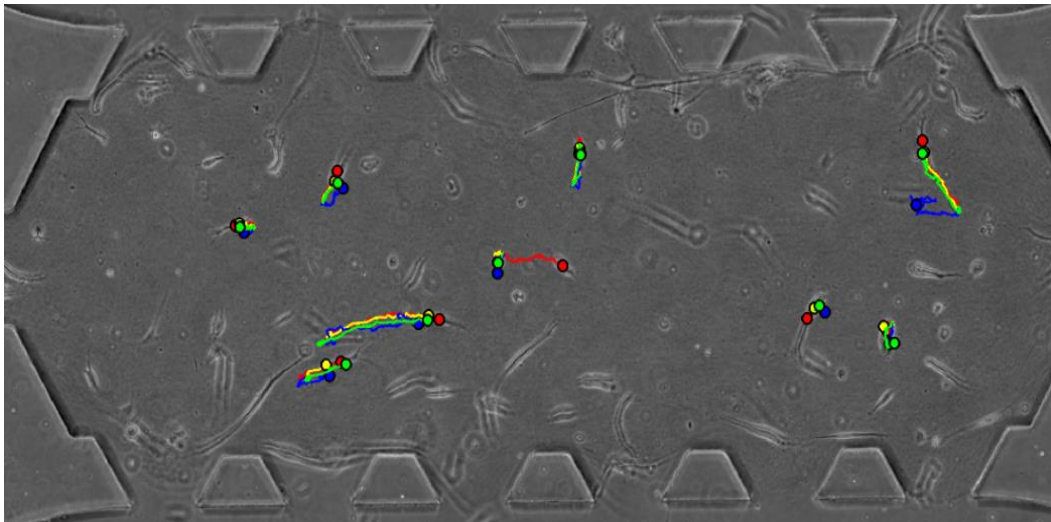


Figure 12. Example of tracking comparing trajectories with different methods in an osteoblasts culture. Red: manual tracking. Green: SegCorr. Blue: Corr, Yellow: MC.

3.1. COMPARISON BETWEEN TRACKING METHODS

Although only 4 methods have been described, each method has been tested with 3 types of image pre-processing (basically background removal), except for the last one (segmentation+correlation+mass center) which has been only tested with raw images, thus making a total of 10 different cases. Henceforth the methods will be referred as follows: mass center (MC), correlation (Corr), segmentation+correlation (SegCorr) and segmentation+correlation+mass center (SegCorrMC) combined with raw images (Raw) and with both background removals (BackG and BackSat).

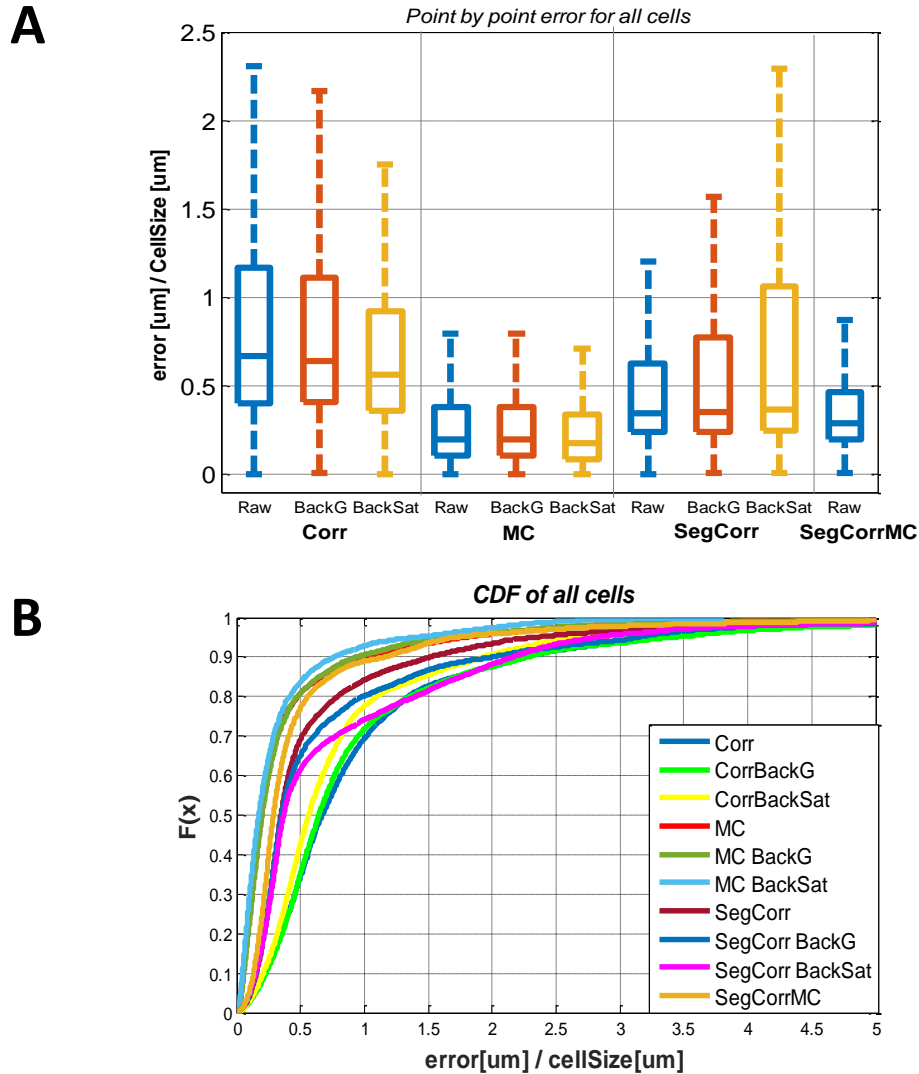


Figure 13. Results of tracking in all cells with all methods implemented A) Boxplot of point by point error by tracking method and background preprocessing. Each color represents one preprocessing method and graph is divided in four parts one for each method. B) Cumulative distribution function of each method for all cells.

In total, almost 7000 points have been evaluated in each method to carry out the study. Two representative graphs are shown in Figure 13 to sum up all the information, as well as a summary table (Table 1). In the first one the boxplot of point-to-point errors have been drawn (showing the median and giving an idea of the dispersion). It is worth reminding that net errors are divided by the cell size so an error of 0.5 corresponds to a cell center that has been marked

at the perimeter of the cell instead of its exact centroid. In the second, the cumulative density function of the data clearly highlights those cases with lower errors (superior lines).

At first glance, a great difference can be seen in the Corr method with respect to the rest, with median values above 0.5 for all the background-subtraction cases and a high dispersion. It must be taken into account that this method was primarily thought for 2D cell assays with homogeneous background. Although modifications have been made, this method works worse than the others, at least for our particular kind of images. In any case, a significant improvement is obtained both in median and deviation when applying the BackSat preprocessing method. With regard to the SegCorr method, considerable improvements have been observed with respect to the application of the simple correlation. In fact, the median error is reduced to a value of 0.35 compared to 0.67 of the Corr method. In the case of SegCorr, there is no improvement in the method with the elimination of background with either of the methods. In fact, the mean, median and deviation values increase when pre-processing the raw images. The median and mean values of the three variants of the MC method are the smallest. In all three cases they are below 0.5 (exact values can be found in table 1). The most successful method is MC BackSat which median is 0.17 and the standard deviation is 0.49.

In this case an outlier has been defined as values greater than 3 times the deviation, and in practice is related to cells that have been lost during the tracking. Cells may get lost in the image because: i) they have changed their z-plane and therefore become blurry (unfocused) decreasing the contrast, ii) the tracking method has followed a different cell because it has divided (proliferated) or crossed paths with another one, iii) the cell has migrated out of the image boundaries. In general, CM method has the lowest number of outliers (142), except for SegCorrBackSat which has only 90 outliers but its mean and deviation is much higher.

Figure 13B shows the cumulative probability of error for each method. In this type of graphs, the ideal would be an elevation as fast as possible, which would mean that the greatest probability of error is around zero. If we analyze all curves we observe four methods that stand out from the rest: MC, MCBackSat, MCBackG and SegCorrMC. In addition to the tracking power of the methods it is important to take into account their computational cost, even though they are all capable of processing a case study with about 10 cells in less than a minute, the truth is that background extraction and correlation calculation are rather heavy tasks. Background extraction requires the initial reading of all images, and what is worse, the whole image area, which is one of the biggest drawbacks in data processing. On the other hand, as the number of cells increases, the correlation task can notably increase the processing time.

	Mean	Med	Std	Max	Nº outliers
Corr	1.00	0.67	1.06	8.98	210
CorrBackG	1.04	0.64	1.25	12.22	212
CorrBackSat	0.86	0.56	0.92	9.78	147
MC	0.43	0.20	0.75	6.97	142
MC BackG	0.43	0.20	0.74	6.97	173
MC BackSat	0.34	0.17	0.49	3.81	151
SegCorr	0.66	0.35	0.92	9.25	181
SegCorrBackG	0.77	0.35	1.10	11.47	219
SegCorrBackSat	0.84	0.37	1.07	9.21	90
SegCorrMC	0.52	0.29	0.75	7.56	186

Table 1. Statistics data of errors for all cells classified by method

3.2. COMPARATIVE STUDY DEPENDING ON CELL TYPE

In this section we will analyze the power of each method for different cell types. In our laboratory migration assays are mainly performed with cardiac, epithelial, stem and osteoblast cells. Hence, this section will be divided in four sub-sections, one for each cell type. The same parameters as in the previous section will be discussed, however, the three correlation methods will be discarded since it has been seen globally that they are much less effective.

Cardiac cells.

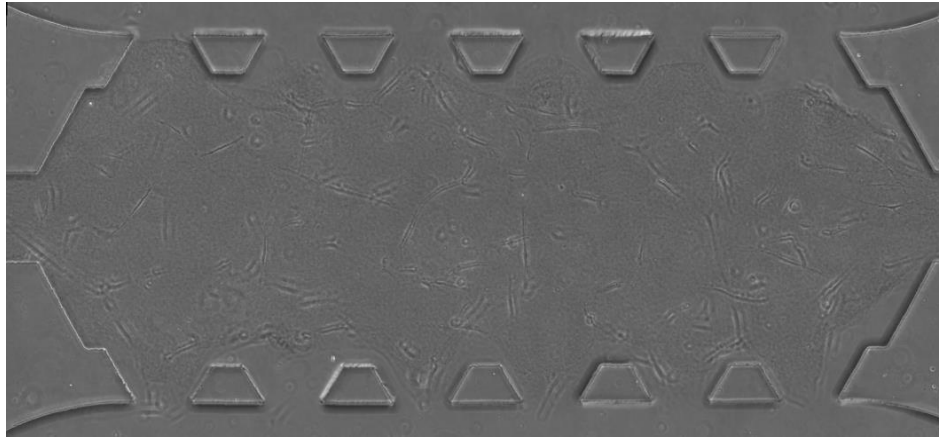


Figure 14. Example of cardiac culture in 3D

Cardiac cells have an elongated appearance and are between 60 and 70 micrometers in size (see Figure 14). Images of cardiac cells that have been analyzed have a fairly high intensity and cells can be easily tracked. Overall, around 1200 points have been automatically obtained. Supplementary material 4 shows a video with the monitoring carried out using the four main methods with raw images. As it can be appreciated in Figure 15, MC and SegCorrMC methods get the best results. Although SegCorrMC method has higher media, the standard deviation and percentile are considerably lower. The exact values are shown in table 2. With regard to the changes between the different pre-processing, there are no significant differences in the results for both the CM and the SegCorr methods, with even better trajectories being obtained using the raw image.

	Mean	Med	Std	Max	Nº outliers
MC	0,40	0,17	0,57	3,00	42
MC BackG	0,40	0,17	0,54	2,97	48
MC BackSat	0,41	0,17	0,62	3,81	33
SegCorr	0,48	0,31	0,57	4,84	32
SegCorrBackG	0,65	0,32	0,81	5,46	34
SegCorrBackSat	0,56	0,32	0,68	5,33	28
SegCorrMC	0,36	0,24	0,42	3,17	41

Table 2. Statistics data of errors for cardiac cells classified by method

On right part of Figure 15 it is easier to compare the error distributions. SegCorrMC method has higher derivate but for higher values of error, that is, it increases faster but later. The other two methods competing with this one are the three MC methods which are occluded

in most of the range. To obtain a more visual result, a video with the different paths has been linked in supplementary material 4.

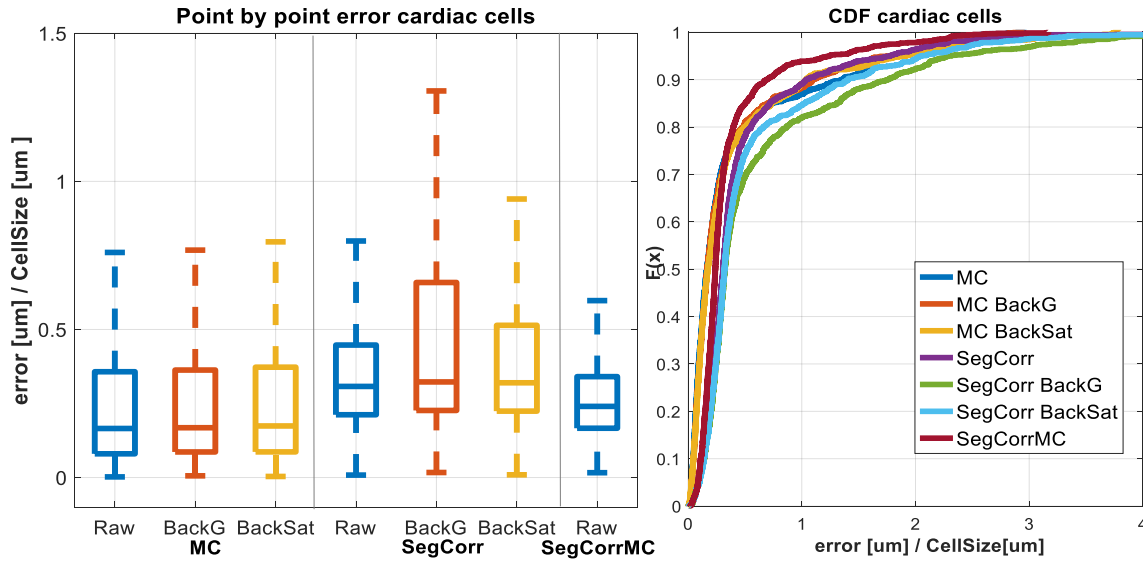


Figure 15. Results of tracking in cardiac cells with MC, SegCorr and SegCorrMC methods A) Boxplot of point by point error by tracking method and background preprocessing. Each color represents one preprocessing method and graph is divided in three parts one for each method. B) Cumulative distribution function of each method for cardiac cells.

Epithelial cells.

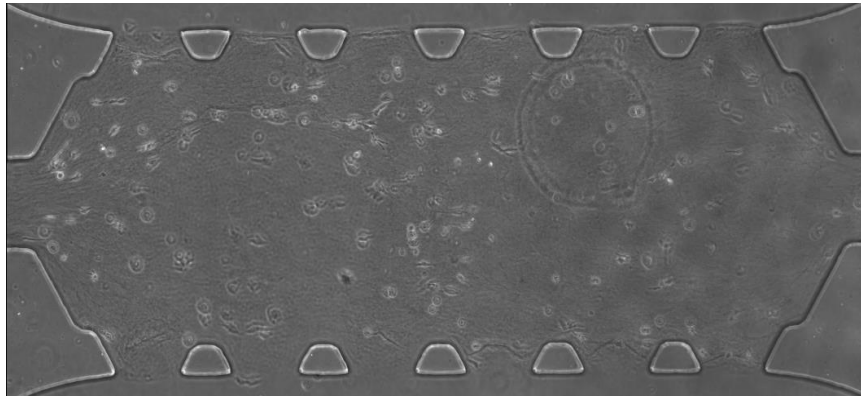


Figure 16. Frame of epithelial cells in 3D culture

Epithelial cells are very different from cardiac ones as shown in Figure 16. Epithelial cells are smaller, around 40μm, and have a very fast division, so it is sometimes difficult to decide which cell to follow. This is reflected in the number of lost cells (representing with number of outliers). It also has the added handicap of being very dark and noisy as shown in the video attached as supplementary material 4. Besides, epithelial cells have a fairly random movement and little displacements. This, coupled with the fact that images have poorer contrast, makes saturated background methods invalid completely because it eliminates most of the cells. Around 2000 points of epithelial cells have been analyzed using five methods: MC, MCBackG, SegCor, SegCorrBackG and segCorrMC, and the results can be seen in Table 3 and Figure 17.

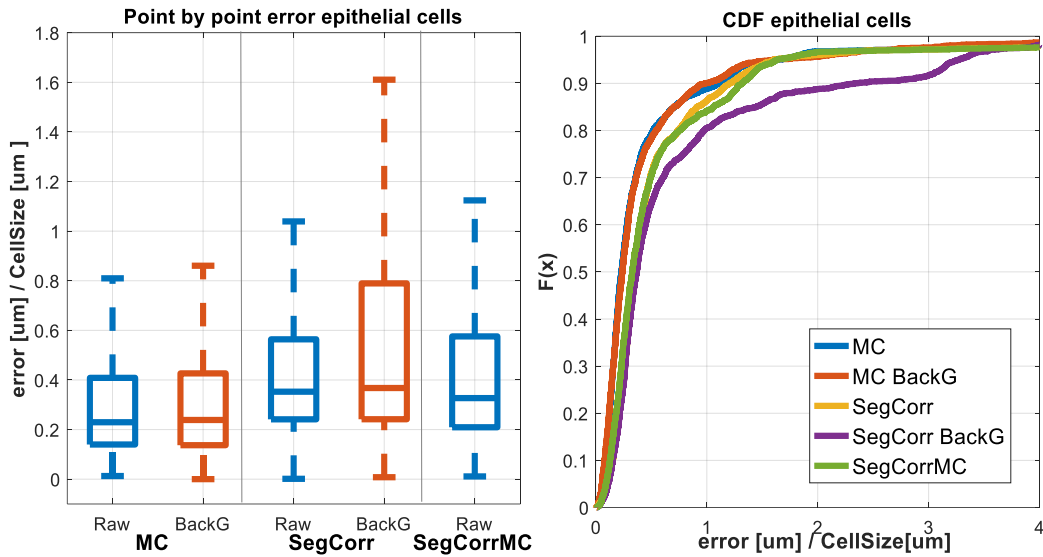


Figure 17. Results of tracking in epithelial cells with MC, MCBackG SegCorr, SegCorrBackG and SegCorrMC methods A) Boxplot of point by point error by tracking method and background preprocessing. Each color represents one preprocessing method and graph is divided in three parts one for each method. B) Cumulative distribution function of each method for epithelial cells.

Epithelial cell test results are worse than those recorded for cardiac cells, as expected by the nature of the images. The mean and median of all methods are above, if in cardiac methods the mean was between 0.36 and 0.65 in the case of epithelial cells are between 0.49 and 0.79. The differences in median values are not as diverse, it means that the dispersion in epithelial cells is bigger. The dispersion is also represented by higher standard deviations. In the case of the SegCorr method, a worsening is observed with the use of the background and in the CM method, hardly any differences are found, although the background method has a lower mean, both have the same median with a value of 0.23. The SegCorrMC method obtains a worse follow up of this type of cells and its median is 0.22 points above that of MC.

	Mean	Med	Std	Max	Nº outliers
MC	0,49	0,23	0,88	6,83	54
MC BackG	0,47	0,23	0,82	6,83	50
SegCorr	0,60	0,35	0,85	6,37	56
SegCorrBackG	0,79	0,37	1,07	6,76	37
SegCorrMC	0,61	0,33	0,92	7.11	54

Table 3 Statistics data of errors for epithelial cells classified by method

Stem cells.

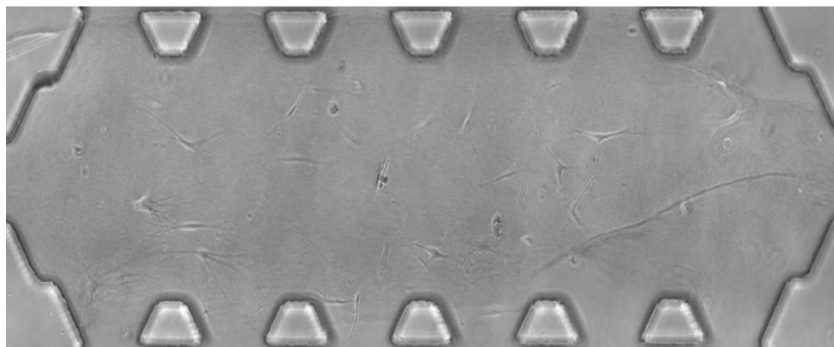


Figure 18. Image of stem cells in 3D culture

Stem cells are very long and thin (about 70-80 μm in length and only 10 in width). A total of 1600 points have been taken from the three trials analyzed. The images are of light intensity and with an uneven background. Additionally, cells present low contrast, which decreases the accuracy of the segmentation methods. One example is shown in Figure 18. The SegCorr method is clearly the least adapted, with values much higher than those obtained in the previous cases. For example, the mean in the SegCorr method is 0.48 for cardiac, 0.60 for epithelial and 0.75 in stem cells. As for the SegCorrCM method, it is maintained in an intermediate state with an average of 0.4, less than the acceptable 0.5. What can be seen in this type of cells is a great adaptation with the MC method, in any of its pre-processing variants, with mean and median values around 0.24 and 0.13, even lower than in the previous cases. Figure 19 shows a slightly better performance of the MCBackSat method on practically overlapping curves.

In supplementary material 4 there is a complete tracking assay of stem cells where most important tracks are represented over time.

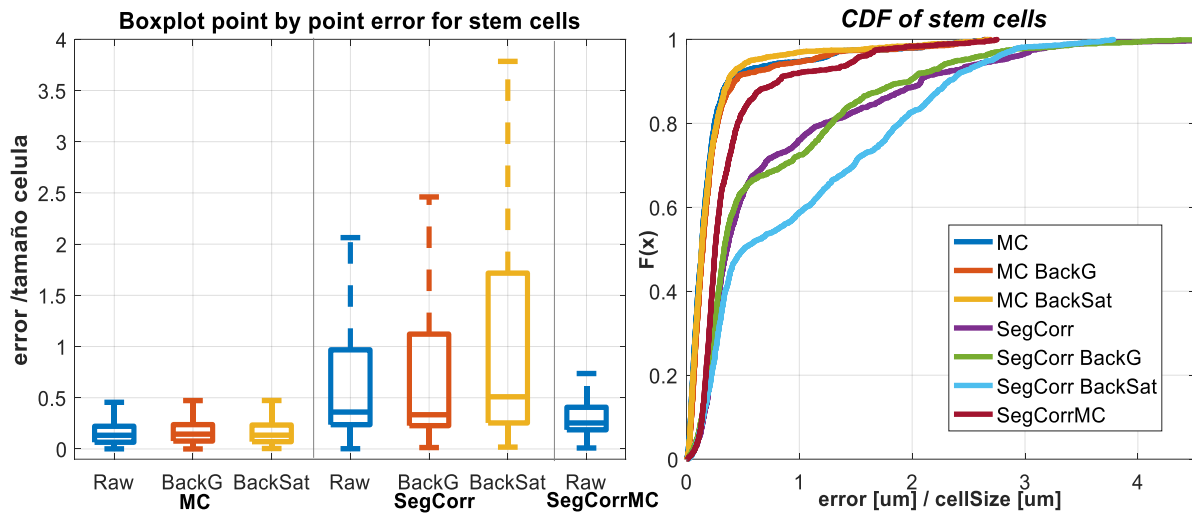


Figure 19. Results of tracking in stem cells with MC, SegCorrBackG with all its preprocessing methods and SegCorrMC . A) Boxplot of point by point error by tracking method and background preprocessing. Each color represents one preprocessing method and graph is divided in three parts one for each method. B) Cumulative distribution function of each method for stem cells.

	Mean	Med	Std	Max	Nº outliers
MC	0,24	0,13	0,39	2,64	42
MC BackG	0,25	0,14	0,40	2,70	42
MC BackSat	0,22	0,13	0,35	2,70	42
SegCorr	0,75	0,36	0,85	4,86	26
SegCorrBackG	0,73	0,33	0,80	4,86	31
SegCorrBackSat	0,99	0,51	0,90	3,78	7
SegCorrMC	0,40	0,25	0,43	2,75	40

Table 4. Statistics data of errors for stem cells classified by method

Osteoblasts.

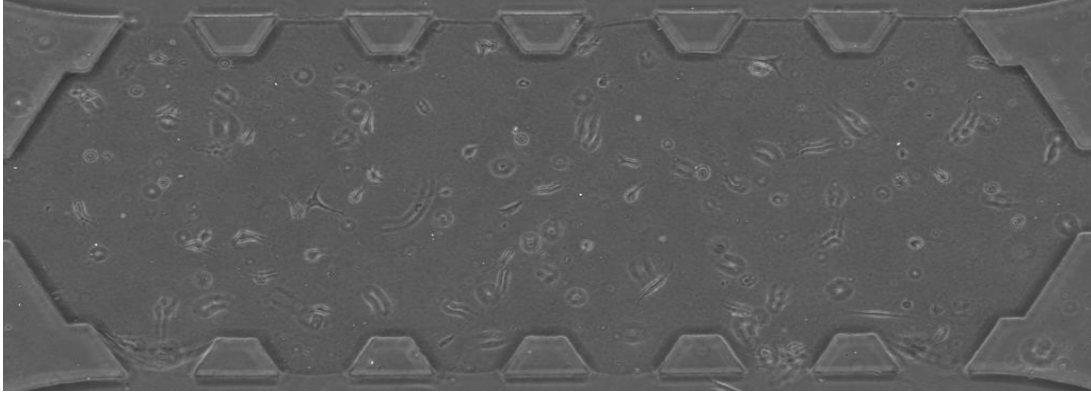


Figure 20. Example image of osteoblast in a 3D culture

Osteoblasts are large cells of about 40 μm that participate in bone regeneration. Despite their irregular shape, that may difficult tracking, osteoblast images have a high contrast, thus making the detection easier (see Figure 20). In terms of tracking accuracy and type of imaging, they are very similar to cardiac cells. All the methods tested presented a median error between 0.2 (for MC and all three different preprocessing) and 0.35 (corresponding to the SegCorr method) (see Table 5). As can be seen on the right part of Figure 21, all the methods get 0.9 of probability density function very closed except for the SegCorrBackG and SegCorrBackSat methods which are slightly worse. In any case, MC methods have the best rises. As in the previous sections, the preprocessing with background elimination does not seem to improve results regarding the use of common filtering. If we compare the MC, SegCorr and SegCorrMC methods we can see a greater stability in the last one, since its percentile is lower, as well as its deviation, with a value of 0.4 with respect to 0.45 of the MC and 0.42 of SegCorr. In this case the number of outliers is also lower, although the difference is minimal. However, the median of the method in which we combine all techniques is significantly superior to the MC method (0.30 compared to 0.2), so probably MC would be more suitable for Osteoblast assays due to the lower computational cost.

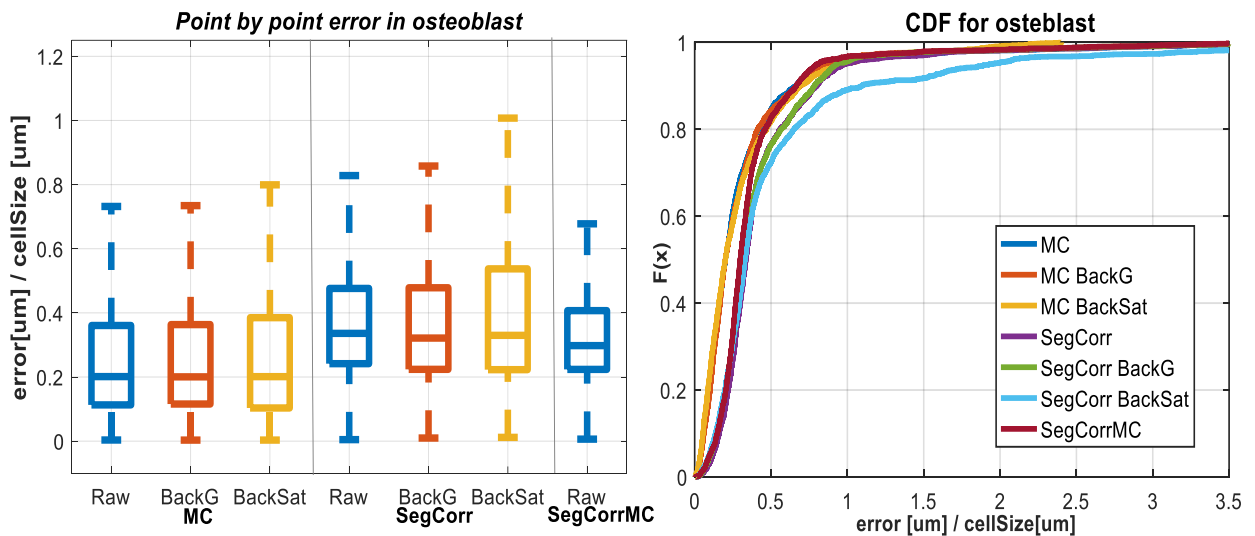


Figure 21. Results of tracking in osteoblasts with MC, SegCorrBackG with all its preprocessing methods and SegCorrMC. A) Boxplot of point by point error by tracking method and background preprocessing. Each color represents one preprocessing method and graph is divided in three parts one for each method. B) Cumulative distribution function of each method for osteoblasts

	Mean	Med	Std	Max	Nº outliers
MC	0,32	0,20	0,45	3,95	43
MC BackG	0,33	0,20	0,44	3,92	40
MC BackSat	0,32	0,20	0,36	2.40	47
SegCorr	0,34	0,35	0,42	3.84	41
SegCorrBackG	0,43	0,32	0,42	3.92	38
SegCorrBackSat	0,56	0,33	0,75	5.27	54
SegCorrMC	0,39	0,30	0,40	3.71	39

Table 5. Statistics data or errors for osteoblast classified by method

3.1. DIFFERENCES BETWEEN 2D AND 3D IMAGES.

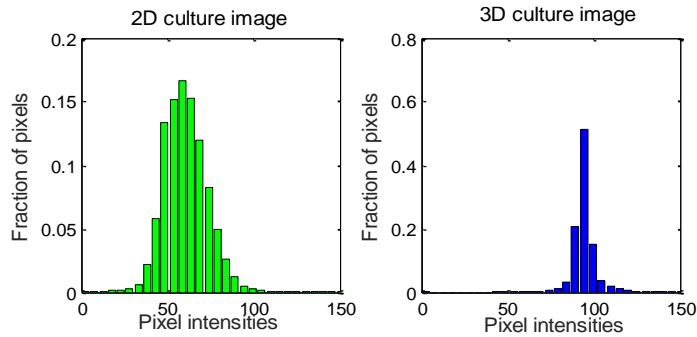
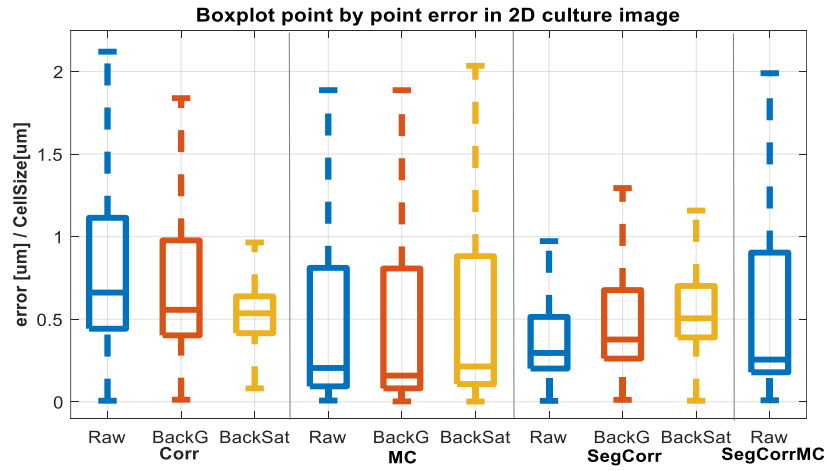


Figure 22. Histogram comparison between images in 2D and 3D culture with 50 bins each histogram and normalized by the total number of pixels of the stack

The assay was carried out with mouse fibroblast in the Center for Medical Physics and Technology of Erlangen. In this case, 200 images (instead of 73 in our assays) were used, and 9 cells were followed. All the implemented methods were tested, including the Correlation ones that had been suppressed in the previous examples due to their poor behavior. The only modification on the algorithms is the cell size, in this case $75\mu\text{m}$. Figure 23 shows the distribution of errors. The Corr method is the only one obtaining a comparable accuracy for 2D than for 3D with an average of 1,0 compared to 0.95 in 3D, and a median of 0.66 as compared to 0.71. By preprocessing the image with the BackSat method, the dispersion is greatly reduced as it can be seen in the percentile, nevertheless, the number of outliers is so far from the other preprocessing methods. It means it follows cells with accuracy but the cells get lost easily. However, in comparison with the other methods very similar results are obtained, the median MC and SegCorr methods are 0.66 and 0.68 respectively. In the MCbackG method the best results are obtained in median and mean but not in deviation which better results are for SegCorr methods especially with BackG preprocessing. Although SegCorr-based methods obtain similar statistical values, if you look at the cumulative distribution functions in the MC curves (almost completely overlapping) there are two steep slopes up to 0.5 and 1.5, while in the SegCorr curve there is a smaller but more continuous slope, this gives us an idea of the histogram profile, with two maximums for MC and one more pronounced in SegCorr. Finally, and in view of the cumulative distribution curves, the methods which achieve the 0.9 of total probability with a minor error are MC, MCBackG, MCBackSat and SegCorr methods which curves have the higher derivative.

A



B

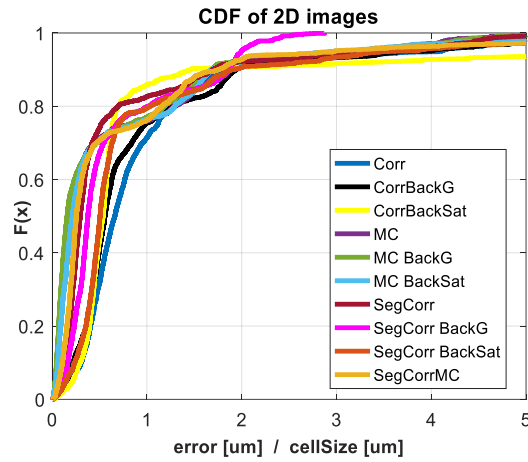


Figure 23. Results of tracking in 2D images with MC, SegCorrBackG with all its preprocessing methods and SegCorrMC. A) Boxplot of point by point error by tracking method and background preprocessing. Each color represents one preprocessing method and graph is divided in three parts one for each method. B) Cumulative distribution function of each method for 2D cultures

	Mean	Med	Std	Max	Nº outliers
Corr	1,00	0,66	1,08	6,15	69
CorrBackG	0,96	0,56	1,11	5,79	68
CorrBackSat	1,06	0,54	1,82	9,68	86
MC	0,66	0,20	1,01	5,29	67
MC BackG	0,64	0,16	1,01	5,28	67
MC BackSat	0,68	0,21	1,06	5,71	55
SegCorr	0,68	0,30	1,02	5,54	71
SegCorrBackG	0,64	0,38	0,62	2,88	14
SegCorrBackSat	0,90	0,26	1,14	6,21	61
SegCorrMC	0,73	0,26	1,16	6,79	57

Table 6. Statistics data of errors for all cells classified by method for a 2D culture image.

Chapter 4

SUMMARY AND CONCLUSIONS

There are many laboratories in which studies of cell migration are carried out with different types of cells and with very diverse objectives such as bone regeneration, cancer metastasis, immune response and so on. For the evaluation of the assays, image analysis and processing is required to extract quantitative data from the experiments. This is why, in many laboratories, specific software is necessary for the study of cell movement in both 2D and 3D cultures, which inevitably entails cell tracking algorithms.

In this project some tracking methods have been developed and tested, comparing them for different cell types and different pre-processing of the input images. Hence, they can be classified into four main groups depending on the algorithm used to associate the cell of a frame to the following: Correlation-based method (Corr), based on the search for the center of masses (MC), based on a segmentation that was used to calculate a correlation between different frames (SegCorrMC) and a method that tries to group all the previous ones (SegCorrMC). Images were pre-processed to obtain a better version of it in three different ways. In the first one, a simple intensity adjustment is used. Since this is not a true pre-processing, this method is called “Raw”. The second one subtracts the background of the image taking into account the median value of each pixel throughout all frames to highlight the cells (BackG). The last one performs a background saturation consisting on set to zero all pixels that are negative when the background is subtracted (BackSat). The resulting trajectories of all these methods are compared against a manual tracking which is considered the ground truth to obtain the errors. For that, the Euclidean distance of each point with respect to the same point in the manual trajectory is used. In order to be able to make a quantitative comparison between values of different cell types, the errors have been divided by the average cell size and the most relevant statistical parameters have been calculated.

Cardiac, epithelial, stem and osteoblast cells have been analyzed in addition to a 2D cultured assay. Table 7 shows a summary of the numerical data obtained, highlighting the most accurate methods for each cell type (green for the best ones and yellow for the acceptable ones).

For cardiac cells the best method is SegCorrMC with 0.36 ± 0.42 ; epithelial cells are really complicated and its result are worse than the others, the most accurate method is MCBackG (0.48 ± 0.82) followed so near for MC method; the best results are for stem (0.22 ± 0.35) and osteoblast (0.32 ± 0.36) which more accurate trajectories are getting with MCBackSat so closed to MC. Finally, and paradoxically, errors obtained for 2D assays were higher than in the others cases although the images were much cleaner (less noisy/blurry) and theoretically easier to analyze. However, the algorithms' parameters were not specifically tweaked for this type of images, so actually it is logical that we obtain poorer results. In any case, in case of necessity, the codes are easily adaptable to analyze 2D cultures. Among all the methods, MC and CorrBackSat showed lower median errors and in this case all Corr methods have better results than in the rest of the cases.

	CARDIAC	EPITHELIAL	STEM	OSTEOBLAST	2D
Corr	0.90 ± 0.82	0.89 ± 0.87	0.85 ± 0.65	0.79 ± 0.76	1.00 ± 1.08
CorrBackG	0.84 ± 0.79	0.97 ± 1.00	0.81 ± 0.68	0.93 ± 0.98	0.96 ± 1.11
CorrBackSat	0.66 ± 0.62	-	0.91 ± 0.75	0.61 ± 0.47	1.07 ± 1.81
MC	0.40 ± 0.57	0.49 ± 0.88	0.24 ± 0.39	0.32 ± 0.45	0.66 ± 1.01
MC BackG	0.38 ± 0.54	0.48 ± 0.82	0.25 ± 0.40	0.33 ± 0.44	0.64 ± 1.01
MC BackSat	0.41 ± 0.62	-	0.22 ± 0.35	0.32 ± 0.36	0.68 ± 1.06
SegCorr	0.48 ± 0.57	0.60 ± 0.85	0.75 ± 0.85	0.44 ± 0.43	0.68 ± 1.02
SegCorrBackG	0.65 ± 0.81	0.79 ± 1.07	0.73 ± 0.80	0.43 ± 0.42	0.64 ± 0.62
SegCorrBackSat	0.56 ± 0.68	-	0.99 ± 0.90	0.56 ± 0.74	0.90 ± 1.14
SegCorrMC	0.36 ± 0.42	0.6 ± 0.92	0.4 ± 0.43	0.39 ± 0.40	0.73 ± 1.16

Table 7. Summary of statistics comparing all methods in all types of cells. Green boxes are the best results and yellow boxes the acceptable ones

In conclusion, we can say that MC, MCBackG and SegCorrMC obtain more accurate trajectories. Actually, the most stable method is mass center-based, moreover it is the less time consuming because despite it is an iterative method the algorithm has very simple steps on it.

Cellular tracking is only the first step, and actually one of the most important, for obtaining data on cell dynamics. Nevertheless, these calculations have no value if they cannot be applied in an easy way. As important is to know the theory as to have a tool to apply it. Therefore, these methods have been included in a semiautomatic platform which uses the methods to automatically track the desired cells, but allows the user to manually correct trajectories at any step, therefore decreasing substantially the errors obtained in this work.

The future work of this project will be to include this and other image processing tools into a cloud service where any laboratory could send its assays and obtain high quality and personalized reports with relevant information.

References

1. Scarpa, E. & Mayor, R. Collective cell migration in development. *J. Cell Biol.* **212**, 143–55 (2016).
2. Masopust, D. & Schenkel, J. M. The integration of T cell migration, differentiation and function. *Nat. Publ. Gr.* **13**, (2013).
3. Brugués, A. *et al.* Forces driving epithelial wound healing. *Nat. Phys.* **10**, 683–690 (2014).
4. Wirtz, D., Konstantopoulos, K. & Searson, P. C. The physics of cancer: the role of physical interactions and mechanical forces in metastasis. *Nat Rev Cancer* **11**, 512–522 (2011).
5. Rosso, F., Giordano, A., Barbarisi, M. & Barbarisi, A. From Cell-ECM interactions to tissue engineering. *J. Cell. Physiol.* **199**, 174–180 (2004).
6. CHAFFEY, N. Alberts, B., Johnson, A., Lewis, J., Raff, M., Roberts, K. and Walter, P. Molecular biology of the cell. 4th edn. *Ann. Bot.* **91**, 401–401 (2003).
7. Ridley, A. J. *et al.* Cell migration: integrating signals from front to back. *Science* **302**, 1704–9 (2003).
8. Parsons, J. T., Horwitz, A. R. & Schwartz, M. A. Cell adhesion: integrating cytoskeletal dynamics and cellular tension. *Nat. Rev. Mol. Cell Biol.* **11**, 633–43 (2010).
9. Bachmann, A. & Straube, A. Kinesins in cell migration. *Biochem. Soc. Trans.* **43**, 79–83 (2015).
10. Ananthakrishnan, R. & Ehrlicher, A. The forces behind cell movement. *Int. J. Biol. Sci.* **3**, 303–17 (2007).
11. Friedl, P. & Wolf, K. Tumour-cell invasion and migration: diversity and escape mechanisms. *Nat. Rev. Cancer* **3**, 362–374 (2003).
12. Driscoll, M. K. & Danuser, G. Quantifying Modes of 3D Cell Migration. *Trends Cell Biol.* **25**, 749–759 (2015).
13. Kraning-Rush, C. M., Carey, S. P., Califano, J. P., Smith, B. N. & Reinhart-King, C. A. The role of the cytoskeleton in cellular force generation in 2D and 3D environments. *Phys. Biol.* **8**, 15009 (2011).
14. Vu, L. T., Jain, G., Veres, B. D. & Rajagopalan, P. Cell migration on planar and three-dimensional matrices: a hydrogel-based perspective. *Tissue Eng. Part B. Rev.* **21**, 67–74 (2015).
15. Stephens, D. J. & Allan, V. J. Light microscopy techniques for live cell imaging. *Science* **300**, 82–6 (2003).
16. Lichtman, J. W. & Conchello, J.-A. Fluorescence microscopy. *Nat. Methods* **2**, 910–919 (2005).
17. Wiedenmann, J., Oswald, F. & Nienhaus, G. U. Fluorescent proteins for live cell imaging: Opportunities, limitations, and challenges. *IUBMB Life* **61**, 1029–1042 (2009).
18. Liu, Z., Tian, L., Liu, S. & Waller, L. Real-time brightfield, darkfield, and phase contrast imaging in a light-emitting diode array microscope. *J. Biomed. Opt.* **19**, 106002 (2014).

19. Meijering, E., Dzyubachyk, O., Smal, I. & van Cappellen, W. A. Tracking in cell and developmental biology. *Semin. Cell Dev. Biol.* **20**, 894–902 (2009).
20. Rohr, K. *et al.* Tracking and quantitative analysis of dynamic movements of cells and particles. *Cold Spring Harb. Protoc.* **2010**, pdb.top80 (2010).
21. Lucchi, A., Smith, K., Achanta, R., Knott, G. & Fua, P. Supervoxel-Based Segmentation of Mitochondria in EM Image Stacks With Learned Shape Features. *IEEE Trans. Med. Imaging* **31**, 474–486 (2012).
22. Dzyubachyk, O., van Cappellen, W. A., Essers, J., Niessen, W. J. & Meijering, E. Advanced Level-Set-Based Cell Tracking in Time-Lapse Fluorescence Microscopy. *IEEE Trans. Med. Imaging* **29**, 852–867 (2010).
23. Chiang, M. *et al.* Analysis of in vivo single cell behavior by high throughput, human-in-the-loop segmentation of three-dimensional images. *BMC Bioinformatics* **16**, 397 (2015).
24. Song, Y. *et al.* Accurate Segmentation of Cervical Cytoplasm and Nuclei Based on Multiscale Convolutional Network and Graph Partitioning. *IEEE Trans. Biomed. Eng.* **62**, 2421–2433 (2015).
25. Cell segmentation in phase contrast microscopy images via semi-supervised classification over optics-related features. *Med. Image Anal.* **17**, 746–765 (2013).
26. Xing, F. & Yang, L. Robust Nucleus/Cell Detection and Segmentation in Digital Pathology and Microscopy Images: A Comprehensive Review. *IEEE Rev. Biomed. Eng.* **9**, 234–263 (2016).
27. Rezatofighi, S. H. *et al.* Multi-Target Tracking With Time-Varying Clutter Rate and Detection Profile: Application to Time-Lapse Cell Microscopy Sequences. *IEEE Trans. Med. Imaging* **34**, 1336–1348 (2015).
28. Magnusson, K. E. G., Jaldén, J., Gilbert, P. M. & Blau, H. M. Global Linking of Cell Tracks Using the Viterbi Algorithm. *IEEE Trans. Med. Imaging* **34**, 911–929 (2015).
29. Maška, M. *et al.* A benchmark for comparison of cell tracking algorithms. *Bioinformatics* **30**, 1609–1617 (2014).
30. Piccinini, F., Kiss, A. & Horvath, P. CellTracker (not only) for dummies. *Bioinformatics* **32**, 955–957 (2016).
31. Bray, M.-A. & Carpenter, A. E. CellProfiler Tracer: exploring and validating high-throughput, time-lapse microscopy image data. *BMC Bioinformatics* **16**, 369 (2015).
32. Chakraborty, A. & Roy-Chowdhury, A. K. Context aware spatio-temporal cell tracking in densely packed multilayer tissues. *Med. Image Anal.* **19**, 149–163 (2015).
33. Sunyer, R. *et al.* Collective cell durotaxis emerges from long-range intercellular force transmission. *Science* **353**, 1157–61 (2016).
34. Moreno-Arotzena, O., Borau, C., Movilla, N., Vicente-Manzanares, M. & García-Aznar, J. M. Fibroblast Migration in 3D is Controlled by Haptotaxis in a Non-muscle Myosin II-Dependent Manner. *Ann. Biomed. Eng.* **43**, 3025–3039 (2015).
35. Movilla, N., Borau, C., Valero, C. & García-Aznar, J. M. Degradation of extracellular matrix regulates osteoblast migration: A microfluidic-based study. *Bone* **107**, 10–17 (2017).
36. Vincent, L. Morphological Grayscale Reconstruction in Image Analysis: Applications and Efficient Algorithms. *IEEE Trans. Image Process.* **2**, (1993).

37. Bolte, S. & Cordelières, F. P. A guided tour into subcellular colocalization analysis in light microscopy. *J. Microsc.* **224**, 213–232 (2006).
38. Shroff, H., Laissue, P. P., Alghamdi, R. A., Tomancak, P. & Reynaud, E. G. Assessing phototoxicity in live fluorescence imaging. *Nat. Publ. Gr.* **14**, (2017).
39. Selinummi, J. *et al.* Bright Field Microscopy as an Alternative to Whole Cell Fluorescence in Automated Analysis of Macrophage Images. *PLoS One* **4**, e7497 (2009).